ISSN 0023-1584, Kinetics and Catalysis, 2020, Vol. 61, No. 4, pp. 575–588. © Pleiades Publishing, Ltd., 2020.
Russian Text © The Author(s), 2020, published in Kinetika i Kataliz, 2020, Vol. 61, No. 4, pp. 526–539.

Palladium-Phosphorus Nanoparticles as Effective Catalysts of the Chemoselective Hydrogenation of Alkynols

N. I. Skripov[a], L. B. Belykh[a, *], T. P. Sterenchuk[a], K. L. Gvozdovskaya[a], V. V. Zherdev[a], T. M. Dashabylova[a], and F. K. Schmidt[a]

[a] *Irkutsk State University, Irkutsk, 664003 Russia*

**e-mail:belykh@chem.isu.ru*

Received September 18, 2019; revised November 8, 2019; accepted December 24, 2019

Abstract—The effect of the composition of the catalytic system and reaction conditions on the properties of phosphorus-modified palladium catalysts in hydrogenations of alkynols was studied. Modification with phosphorus increased the activity and turnover number of palladium catalysts in the hydrogenation of the model compound 2-methyl-3-butyn-2-ol (MBY) without any reduction in the selectivity to 2-methyl-3-butene-2-ol at 95–98% MBY conversion. The promoting effect of phosphorus on the properties of the palladium catalyst is caused not only by an increase in the particle size, but also, probably, by a change in the energy of interaction of reagents with the active sites. Hypotheses on the nature of the carriers of catalytic activity in Pd–P particles were discriminated using kinetic methods with the differential selectivity of catalytic systems as the main measured parameter under the conditions of competition between two alkynols. The hydrogenation of acetylenic alcohols involves only one of the two potentially active forms in Pd–P nanoparticles—Pd(0) clusters, whereas the hydrogenation of the resulting allyl alcohols involves both Pd(0) clusters and palladium phosphides.

Keywords: hydrogenation, palladium, phosphorus, nanoparticle, phosphide, cluster, 2-methyl-3-butyn-2-ol, 3-methyl-1-pentyn-3-ol, activity, differential selectivity

DOI: 10.1134/S0023158420030209

INTRODUCTION

The selective hydrogenation of multiple bonds, including the chemoselective hydrogenation of alkynes to alkenes [1–4] and of alkynols [5, 6] or unsaturated carbonyl compounds [7] to allyl alcohols without their further hydrogenation to alkanes or alkanols, respectively, is an important reaction in chemical industry; it is mainly used in the production of polymers, pharmaceuticals, fat-soluble vitamins (e.g., E and K) and agrochemicals. Thus, the level of phenylacetylene in the monomer—styrene with a polymerization degree of purity—should be below 10 ppm [8]. In the synthesis of many pharmaceuticals, vitamins, flavors, and agrochemicals, however, the catalysts developed over 60 years ago are used [1]. The typical catalysts for selective hydrogenations are most often obtained by "partial poisoning of the active metal" (Pd, Pt, Rh, or Ni); the metal that is active in catalysis is protected and selectively deactivated by various compounds: Pb, V, Cu, Ag, CO, quinolone, etc. [1]. Increased selectivity is generally achieved at a sacrifice of catalytic activity, which is reduced. The presence of toxic elements (primarily, Pb) in the chemoselective catalyst and low catalytic activity impose serious restrictions on future applications of these materials. In connection with modern environmental safety standards [9], the goal is to create highly selective and environmentally more friendly catalysts that meet the sustainable development strategy and are characterized by a reasonable proportion of selectivity and activity [10]. Therefore, studies in this field have gained a new impetus in the last decade [1].

Modern approaches aimed at creating selective catalysts of chemoselective hydrogenation of alkynes and alkynols are based on the size and shape control of transition metal nanoparticles [10–12]; isolation of active sites on the surface of hybrid materials and development of catalysts based on individual palladium atoms [1, 13]; the use of new bimetallic alloys [5, 14–16]; and surface modification of the active component of the catalyst [6, 17] or support [18].

The palladium catalysts of hydrogenation are generally modified by Lewis bases [1] and alkali metal cations in the form of salts and bases [6]. The introduction of nitrogen-containing Lewis bases leads to an increase in selectivity due to a decrease in catalytic

Abbreviations: DMF, N,N-dimethylformamide; MBY, 2-methyl-3-butyn-2-ol; MPY, 3-methyl-1-pentyn-3-ol; MBE, 2-methyl-3-butene-2-ol; MBA, 2-methylbutan-2-ol; XRD analysis, X-ray powder diffraction analysis; XPS, X-ray photoelectron spectroscopy; GLC, gas-liquid chromatography; TON, turnover number; TOF, turnover frequency.

activity (blocking of active sites) [1], while alkali metal cations at certain concentrations promote both selectivity and activity of palladium catalysts in the hydrogenation of alkynols [6]. Sodium and potassium hydroxides facilitate the reduction of Pd(II) precursors to Pd(0). Alkali metal cations can interact with the surface of Pd nanoparticles, leading to site separation and changing the adsorption energy of reagents, and they also affect the mobility of Pd nanoparticles on solid supports, preventing the sintering during the heat treatment. The activity of heterogeneous palladium catalysts modified with alkali metal cations in the hydrogenation of alkynols does not exceed 426 min^{-1} at rather high (90°C) temperatures [6].

Tertiary, secondary, and primary phosphines, unlike nitrogen-containing Lewis bases, undergo degradation in the coordination sphere of Pd(0), which gives rise to polynuclear palladium complexes with phosphide, phosphynidene ligands, and even palladium phosphides [19, 20]. Taking into account the formation of palladium phosphides during the formation and functioning of active particles based on palladium phosphine complexes, we proposed the most reactive form of elemental phosphorus—white phosphorus—as a modifier instead of phosphines, in order to develop effective catalysts of hydrogenation [21].

The reduction of palladium compounds with hydrogen in the presence of P_4 under mild conditions makes it possible to obtain highly dispersed palladium catalysts, whose particles contain Pd(0) clusters and palladium phosphides. The size, composition, and state of the surface layer of particles can be varied by varying the P : Pd ratio [21], the acido ligand at palladium [22, 23], or the solvent [24]. Of the two chemical forms of palladium (Pd^0, $Pd^{\delta+}$), Pd(0) prevails on the surface of nanoparticles at low initial P : Pd ratios (≤0.3); its electron binding energy is 0.7 eV lower than that of bulk palladium [25]. As the hydrogenation of alkynols is a size-sensitive reaction [11, 12], the abovementioned physical characteristics of Pd–P nanoparticles must have a positive effect on their properties in the hydrogenation of alkynols.

In order to develop effective catalysts of the chemoselective hydrogenation of acetylenic compounds and determine the nature of catalytic activity carriers, we studied the hydrogenation of 2-methyl-3-butyn-2-ol and the competitive hydrogenation of alkynols under the action of Pd–P particles formed by the low-temperature method.

EXPERIMENTAL

Materials

The solvents (benzene, N,N-dimethylformamide) were purified by the standard procedures [26]. N,N-Dimethylformamide (DMF) was kept over anhydrous copper sulfate until a green solution was obtained, for dehydration and removal of amine impurities; then it was subjected to two vacuum distillations (8 Torr) at a temperature of up to 42°C. For deeper drying, benzene was additionally distilled over $LiAlH_4$ using a distillation column. The solvents were stored in an argon atmosphere in sealed ampules over 4A molecular sieves.

Palladium *bis*-(acetylacetonate) $Pd(acac)_2$ was prepared by the procedure described in [27] followed by recrystallization from acetone. Palladium diacetate ($Pd(OAc)_2$) and palladium dichloride ($PdCl_2$) ((chemically pure)) were used without additional purification.

White phosphorus was mechanically cleaned from the surface oxidation products and washed in anhydrous benzene immediately before use. A solution of white phosphorus in benzene was prepared and stored in an inert atmosphere in a finger-type vessel, which was previously evacuated and filled with argon.

2-Methyl-3-butyn-2-ol (MBY) (Sigma-Aldrich, >98%) and 3-methyl-1-pentyn-3-ol (MPY) (Sigma-Aldrich, >98%) were used without additional purification. Phenylacetylene was kept over previously calcinated calcium dichloride for 2 weeks and distilled over calcium hydride (40°C/10 Torr). Styrene was purified by shaking it with a 5% alkali solution until a portion of alkali became colorless. Then it was washed with distilled water, dried over anhydrous calcium chloride, and distilled in vacuum (32°C/10 mmHg).

Triethylaluminum ($AlEt_3$) (Sigma-Aldrich) was distilled in vacuum, collecting a fraction boiling at 48–49°C/1 Torr, and used as a solution in benzene. ^1H NMR: $\delta(CH_3)$ = 1.22 ppm, (t, 3H, ^1J = 8.24 Hz); $\delta(CH_2)$ = 0.45 ppm (q, 2H, ^1J = 8.24 Hz).

Examples of Experiments

Alkynols were hydrogenated in a thermostatted glass vessel of the duck type at 30°C and initial hydrogen pressure of 2 atm in the presence of a Pd–P catalyst formed in situ.

A solution of phosphorus in benzene (0.1×10^{-5}–1.0×10^{-5} mol based on the atomic form of phosphorus) (1 mL) was added dropwise to a solution of $Pd(acac)_2$ (0.00304 g, 1×10^{-5} mol) in DMF (9 mL) placed in a thermostatted duck vessel. The solution was stirred for 7 min at room temperature. Then the temperature was raised to 80°C, and the reaction mixture was stirred in hydrogen for 40–45 min up to quantitative conversion of $Pd(acac)_2$. The resulting black and brown colloidal solution was cooled to 30°C, a hydrogen pressure of 2 atm was created, and the 2-methyl-3-butyn-2-ol substrate was syringed through a teflon stopper with a rubber gasket. MBY was hydrogenated with vigorous stirring, precluding the reaction in the diffusion region, while periodically collecting aliquots of reaction mixture for GLC analysis.

The catalytic systems were formed in the same way at $Pd(acac)_2$ concentrations higher than 1 mmol/L. The properties of Pd–P particles at catalyst concentrations of 0.25 and 0.5 mmol/L were studied by diluting the preformed catalyst system ($C_{Pd(acac)_2} = 1$ mmol/L). The catalytic experiments using other palladium precursors ($PdCl_2$, $Pd(OAc)_2$) were performed in a similar way. The differences were in the temperature and time of catalyst formation. In the case of $PdCl_2$ and $Pd(OAc)_2$, the catalyst systems formed in hydrogen at 30°C for 5 min.

The hydrogenation of alkynols proceeds in two stages. At the first stage, the triple bond is predominantly hydrogenated; at the second stage, the resulting allyl alcohol is reduced to saturated alcohol. The amount of the product of complete hydrogenation (alkanol) at the first stage was up to 5%. Therefore, the reaction rate $r\left(\text{mol}_{H_2}/\text{min}\right)$ at each stage was determined from the kinetic curve in the following way. The rate of MBY hydrogenation to allyl alcohol was calculated from the slope of the straight sections of the curves in the hydrogen absorption range 0.1–0.5 mol H_2 per mol MBY. The rate of hydrogenation of allyl alcohol to saturated alcohol was found from the slope of the straight sections of the curves in the hydrogen absorption range 1.1–1.3 mol H_2 per mol MBY. The selectivity of Pd–P catalysts for 2-methyl-3-butene-2-ol was calculated at 95–98% conversion of the starting acetylene alcohol. In order to determine the highest TON and the stability of the Pd–P catalyst, hydrogenation was repeated by introducing an aliquot of fresh substrate in the reaction vessel after the hydrogenation of the previous portion of MBY to 2-methylbutan-2-ol was completed.

The competitive hydrogenation of alkynols in the presence of Pd–P particles obtained from $Pd(acac)_2$ and P_4 in hydrogen was performed as in the case of the noncompetitive hydrogenation of alkynols. For this, a mixture of alkynols: 2-methyl-3-butyn-2-ol (MBY) (3.3535 mmol, 0.31 mL) and 3-methyl-1-pentyn-3-ol (MPY) (3.3644 mol, 0.38 mL) was injected with a syringe into a colloidal solution of Pd–P particles formed in situ (as described above) and hydrogenated with vigorous stirring. The reaction was monitored by GLC analysis of the intermittently collected samples.

The dispersion (D_{TEM}) and TOF of Pd black and Pd–P particles were calculated by the following equations:

$$D_{TEM} = \frac{6M_{Pd}}{\rho_{Pd} d_{TEM} A_{Pd} N_A}, \quad (1)$$

where M_{Pd} is the atomic mass of Pd (g/mol); A_{Pd} is the surface area of the Pd atom ($m^2_{Pd\ surf}/atom_{Pd\ surf}$); ρ is the density of palladium; N_A is the Avogadro number; and d_{TEM} is the surface-average particle diameter;

$$d_{TEM} = \frac{\sum_i n_i d_i^3}{\sum_i n_i d_i^2}, \quad (2)$$

where n_i is the number of particles with a diameter d_i;

$$\text{TOF} = \frac{A}{D_{TEM}}, \quad (3)$$

where A is the catalytic activity calculated based on all palladium (mol of substrate (mol of Pd_{tot} min)$^{-1}$); and D_{TEM} is the dispersity determined from the transmission electron microscopy data.

The above approach was used only for the Pd–P particles (initial ratio P : Pd ≤ 0.3) whose volume and surface were enriched with palladium Pd(0) according to the XRD and XPS data [25].

Methods of Investigation

The UV spectra of the catalyst solutions were recorded on an SF-2000 spectrophotometer (Spektr, Russia) in quartz cells with an absorbing layer thickness of 0.1 cm. The conversion of $Pd(acac)_2$ was monitored according to the 330 nm absorption band ($\varepsilon_{330} =$ 10 630 L cm^{-1} mol^{-1}).

The hydrogenation products were analyzed by GLC on a Crystal 5000 chromatograph (Chromatec, Russia) equipped with a 30 m long capillary column (phase: 5% diphenyl, 95% dimethylpolysilphenylene siloxane) and a flame ionization detector (FID) by the internal standard method using temperature programming: 100°C (1.5 min), 270°C (10 min), heating rate 30°C/min. The pressure of the carrier gas (nitrogen) was 20 kPa.

The hydrogenation products were additionally analyzed on a GCMS-QP2010 Ultra chromato-mass spectrometer (Shimadzu, Japan) with a 30 m long GsBP-5MS capillary column; the phase was poly(5% diphenyl, 95% dimethylpolysilphenylene siloxane). Ionization was performed by electron impact; the ionization energy was 70 eV. The obtained mass spectra were compared with published data (Wiley, NIST, NIST05 databases).

The TEM images were obtained on a Tecnai G^2 electron microscope (FEI, United States) with an accelerating voltage of 200 kV. A drop of the reaction solution was applied to a carbonized copper grid and dried in a box in an inert atmosphere at room temperature. The images were recorded using a CCD camera (Soft Imaging System, Germany). To find the average particle size, a section containing at least 100–150 particles was processed.

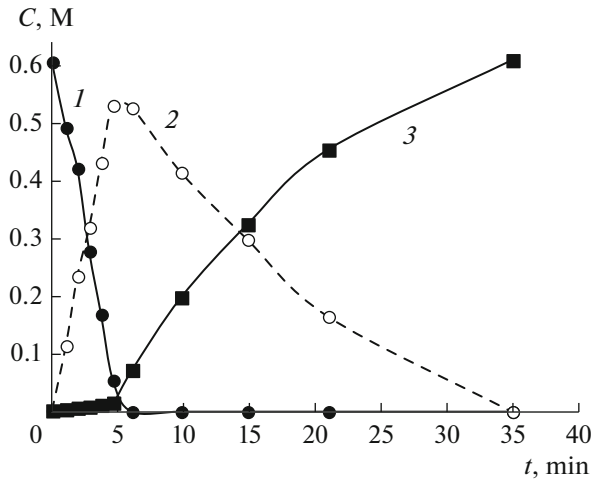

Fig. 1. Kinetic curves of hydrogenation of (*1*) 2-methyl-3-butyn-2-ol and (*2*), (*3*) formation of (*2*) 2-methyl-3-butene-2-ol and (*3*) 2-methylbutan-2-ol in the presence of Pd–P particles; P : Pd = 0.3. Reaction conditions: C_{Pd} = 0.25 mmol/L, C_{MBY} = 0.598 mmol/L, T = 30°C, P_{H_2} = 2 atm.

RESULTS AND DISCUSSION

Hydrogenation of 2-methyl-3-butyn-2-ol in the presence of Pd black and Pd–P particles in DMF is an example of a typical sequential reaction. At the first stage of the reaction (before the absorption of 1 mol H_2 per mol MBY), 2-methyl-3-butyn-2-ol is predominantly hydrogenated to 2-methyl-3-butene-2-ol; at the second stage, the product of hydrogenation of 2-methyl-3-butene-2-ol—2-methylbutan-2-ol—forms (Fig. 1). The products of dimerization of alkynol C_{10} and hydrogenation of the resulting dimer (2,7-dimethyl-3,5-octadiyn-2,7-diol to 2,7-dimethyl-5-octen-3-yn-2,7-diol) were detected in trace amounts by chromato-mass spectrometry and GLC. The products of isomerization of 2-methyl-3-butyn-2-ol to unsaturated aldehyde were absent.

The activity of Pd–P particles in the hydrogenation of 2-methyl-3-butyn-2-ol depends on the composition of the catalytic system and reaction conditions. As a result of the modification of the palladium catalyst with phosphorus introduced before the stage of the reduction of $Pd(acac)_2$ with hydrogen, the rates of hydrogenation of both the triple bond of MBY and the double bond of the 2-methyl-3-butene-2-ol product increase without any decrease in selectivity for allyl alcohol over the whole range of P : Pd = 0.1–1 at 99–98% conversion of the substrate (Fig. 2). Even when small amounts of elemental phosphorus are introduced (P : Pd = 0.1), the activity of Pd–P particles (A) calculated for all palladium increases from 58.5 to 185 min^{-1}, i.e., almost threefold compared with that of Pd black (Fig. 2a). At a $Pd(acac)_2$ concentration of 1 mmol/L, the greatest promoting effect of phosphorus is observed at a ratio of P : Pd = 0.3: the activity of Pd–P particles in MBY hydrogenation is 285 min^{-1} (Fig. 2a).

Under the isothermal conditions of the process, the activity of Pd–P particles is determined not only by the P : Pd ratio, but also by hydrogen pressure and MBY and palladium precursor concentrations (Fig. 3). The rate of hydrogenation of the MBY triple

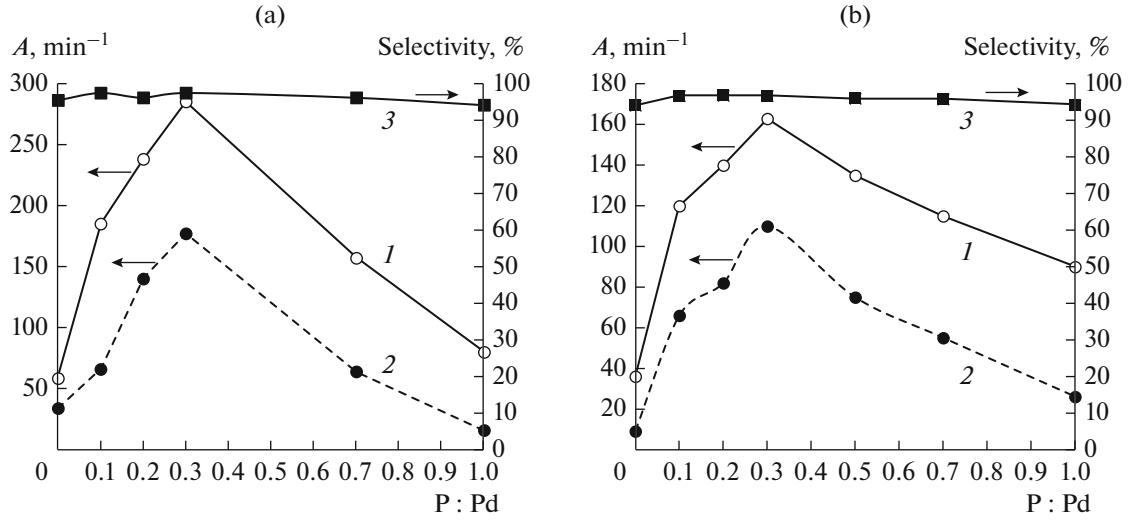

Fig. 2. Effect of the phosphorus modifier on the (*1*, *2*) activity and (*3*) MBE selectivity of Pd–P nanoparticles in hydrogenation of (*1*) 2-methyl-3-butyn-2-ol and (*2*) 2-methyl-3-butene-2-ol at a $Pd(acac)_2$ concentration of (a) 1 or (b) 2 mmol/L. Reaction conditions: $\nu_{MBY} = 6.64 \times 10^{-3}$ mol, DMF solvent, 10 mL, T = 30°C; P_{H_2} = 2 atm. The selectivity was measured at 97–98% conversion of MBY.

bond (r_1) depends linearly on the hydrogen pressure (Fig. 3a), and the dependence of the reaction rate on the MBY substrate concentration passes through a maximum (Fig. 3b). The MBY hydrogenation rate nonlinearly increases when the $Pd(acac)_2$ concentration increases from 0.25 to 5 mmol/L, reaching a plateau at $C_{Pd(acac)_2}$ = 2 mmol/L (Fig. 3c). The dependence of the activity of Pd–P particles on $C_{Pd(acac)_2}$ in the indicated range of concentrations is antibatic (Fig. 3c). At an optimum concentration of $Pd(acac)_2$ (0.25–0.5 mmol/L), the activity of Pd–P particles in MBY hydrogenation reaches 450 min^{-1} at 30°C and P_{H_2} = 2 atm. In their activity in MBY hydrogenation, the Pd–P particles surpass the palladium clusters in the form of a cube or cuboctahedron with sizes of 6 and 5.5 nm ($A_{Pd\ total}$ = 153 and 135 min^{-1}, respectively; T = 60°C, P_{H_2} = 3 atm) [10], bimetallic alloys Pd_7Bi/SiO_2 ($A_{Pd\ total}$ = 12.6 min^{-1}; T = 50°C, P_{H_2} = 1 atm) [14], and $PdZn/TiO_2$ ($A_{Pd\ total}$ = 180 min^{-1}; T = 40°C, P_{H_2} = 1 atm) [14] and are comparable to Ziegler type systems (Table 1). For Ziegler type systems, as well as for Pd–P particles, the catalytic activity increases after dilution of the $Pd(acac)_2$–n $AlEt_3$ system (n = 4, 6) (from 2 to 0.5 mmol/L) (Table 1). The reasons for the effect of dilution on the activity of Pd–P particles and palladium nanoclusters in Ziegler systems, in our opinion, may be as follows.

According to the TEM data, the Pd–P nanoparticles are aggregates of particles (Figs. 4b–4e), while the palladium nanoclusters in Ziegler systems are represented by individual high-contrast particles (Fig. 4f). The reason for the aggregative stability of palladium nanoclusters is their stabilization with $AlEt_2(acac)$ and $AlEt_3$ [28–30]. The inhibitory effect of organoaluminum compounds as a result of adsorption on the palladium active sites was previously proved experimentally [29, 30]. In view of this, the increase in the activity of Ziegler systems in the hydrogenation of MBY after dilution of the reaction solution is mainly due to the elimination of the inhibitory effect of the stabilizers ($AlEt_2(acac)$, $AlEt_3$) as a result of hydrolysis of the surface compounds with water impurities in the solvent. The reason for the effect of dilution on the activity of Pd–P particles may be prevented aggregation of particles, which is known to occur by a second order reaction [28]. The reaction occurring in the kinetic region was proved by additional experiments.

The introduction of phosphorus before the stage of $Pd(acac)_2$ reduction with hydrogen significantly increases not only the activity but also the productivity of palladium catalysts. In MBY hydrogenation under the action of the Pd–P catalyst (P : Pd = 0.5), TON is almost two times higher (10 650 mol MBY per mol Pd) than that of Pd black (5470 mol MBY per mol Pd) (Fig. 5).

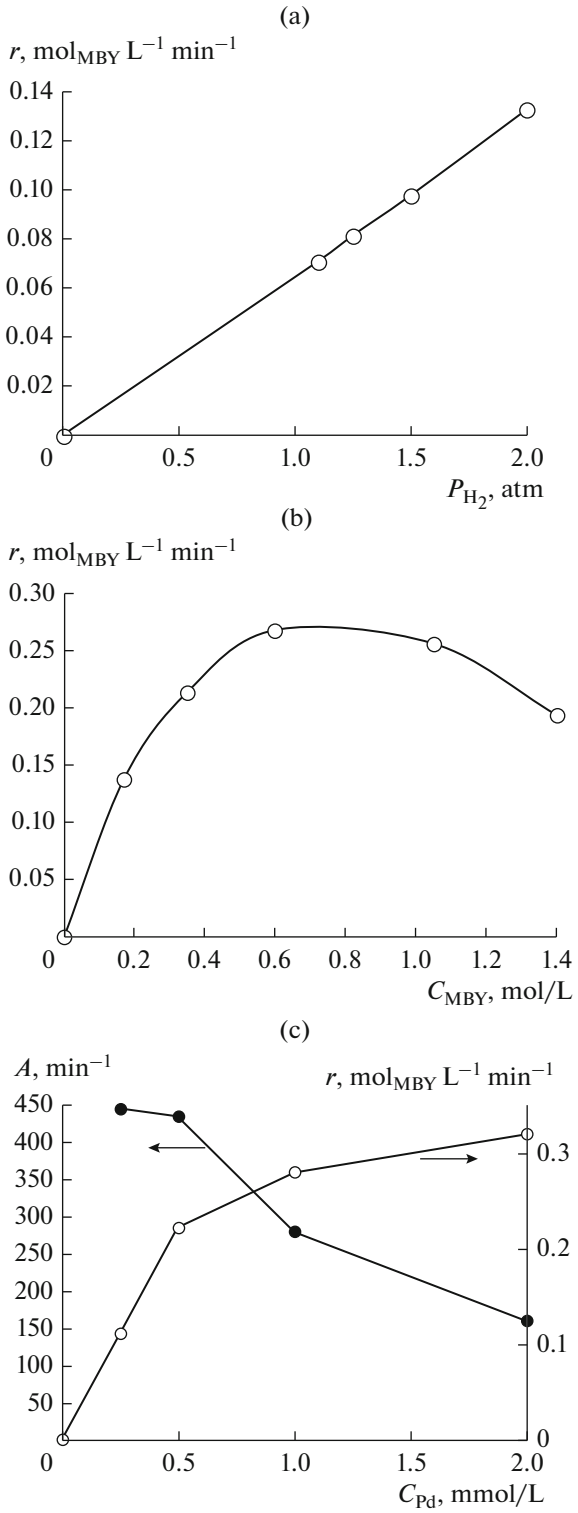

Fig. 3. Dependence of the hydrogenation rate (r) of 2-methyl-3-butyn-2-ol or activity (A) on the (a) hydrogen pressure and (b), (c) concentration of the (b) substrate and (c) $Pd(acac)_2$ in the presence of Pd–P particles (P : Pd = 0.3). Reaction conditions: (a) C_{Pd} = 0.5 mmol/L, C_{MBY} = 0.598 mol/L, T = 20°C; (b) C_{Pd} = 0.5 mmol/L, T = 30°C, P_{H_2} = 2 atm; (c) $\nu_{MBY} = 6.64 \times 10^{-3}$ mol, T = 30°C, P_{H_2} = 2 atm, DMF solvent, 10 mL.

Table 1. Catalytic properties of Ziegler type systems $Pd(acac)_2$–$nAlEt_3$ in the hydrogenation of 2-methyl-3-butyn-2-ol*

$AlEt_3$: Pd	C_{Pd}, mmol/L	Activity (A), min^{-1}		$A_1 : A_2$	Conversion, %	Selectivity for MBE, %
		A_1 −C≡C−	A_2 −C=C−			
4	2	194	441	0.4	94.2	93.9
6	2	184	373	0.5	95.8	92.7
4	1	395	528	0.7	91.8	95.6
4	0.5	370	772	0.5	96.6	94.1
6	0.5	367	744	0.5	97.8	93.7
10	0.5	332	557	0.6	97.1	92.9

* Reaction conditions: $\nu_{MBY} = 6.64 \times 10^{-3}$ mol; toluene solvent, volume 10 mL, $T = 30°C$; $P_{H_2} = 2$ atm.

The replacement of the acetylacetonate ligand at palladium by acetate has almost no effect on the properties of Pd–P nanoparticles in the hydrogenation of 2-methyl-3-butyn-2-ol (Table 2). The lower activity of Pd–P particles obtained from $PdCl_2$ is the result of poisoning of the surface palladium atoms by chloride anions that formed as a result of hydrogenolysis. Thus, phosphorus mainly affects the activity and productivity of the palladium catalyst in the hydrogenation of 2-methyl-3-butyn-2-ol, while retaining high selectivity at 96–98% conversion of the substrate.

The promoting effect of phosphorus on the activity of Pd–P nanoparticles in the hydrogenation of 2-methyl-3-butyn-2-ol may be the consequence of the increased proportion of active sites and/or the formation of new, more active catalyst sites. To distinguish between these two factors, it is necessary, first of all, to take into account the fraction of surface atoms in Pd black, palladium clusters in Ziegler systems, and

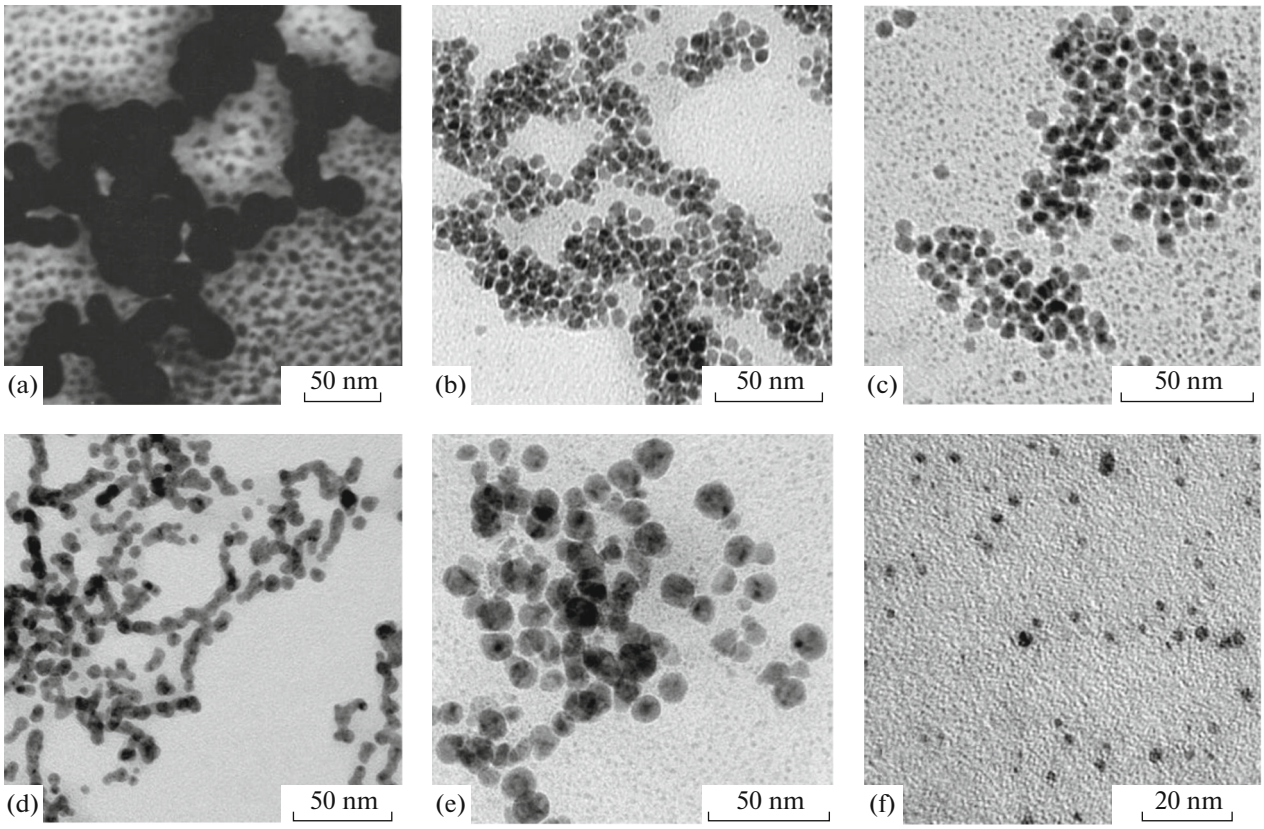

Fig. 4. TEM images of the catalysts: (a) Pd black; (f) $Pd(acac)_2$–$4AlEt_3$ system, $C_{Pd} = 5$ mmol/L; (b) Pd–P particles formed in hydrogen, P : Pd = 0.3; (c) P : Pd = 1.0, $C_{Pd} = 1$ mmol/L; (d) P : Pd = 0.1, $C_{Pd} = 1$ mmol/L; (e) $C_{Pd} = 2$ mmol/L.

Pd–P particles. The results of TEM determination of the sizes of Pd black formed from $Pd(acac)_2$ in hydrogen, palladium clusters in Ziegler systems, and Pd–P particles depending on the initial $Pd(acac)_2$ concentration and the amount of introduced modifier are presented in Table 3. The particle size of the Pd–P catalyst decreased almost fourfold compared with the size of Pd black (Fig. 4). The number average size of Pd–P particles changed slightly when the P : Pd ratio increased: from 5.9 ± 1.04 (P : Pd = 0.1) to 5.5 ± 0.92 (P : Pd = 0.3) and 5.3 ± 1.01 nm (P : Pd = 1.0). The size of Pd–P particles and Pd black increases with the concentration of the precursor ($Pd(acac)_2$). For the Pd–P catalyst (P : Pd = 0.1), it increases from 5.9 ± 1.04 nm (C_{Pd} = 1 mmol/L) to 10.7 ± 2.3 nm (C_{Pd} = 2 mmol/L) (Fig. 4).

The turnover frequencies of palladium catalysts calculated for the surface palladium atoms are presented in Table 3. The highest TOF values characteristic of Pd black and Pd–P particles in MBY hydrogenation differ 1.8-fold ($TOF_{Pd-P} : TOF_{Pd\ black} = 1.8$). According to TOF, the Pd–P particles surpass not only palladium nanoclusters in the form of a cube (TOF = 918 min^{-1}), octahedron (TOF = 1050 min^{-1}), and cuboctahedron (TOF = 876 min^{-1}) [10], which are close in size, but also Ziegler type systems (Table 3).

Additional experiments on hydrogenation of phenylacetylene and styrene in the presence of Pd–P particles showed similar results (Table 3). According to TOF in hydrogenation of both phenylacetylene and styrene, Pd–P particles surpass both Pd black and palladium nanoclusters in Ziegler systems. The significantly higher TOF values of Pd–P particles (TOF = 2380 min^{-1}) relative to TOFs for Pd black (Table 3) and palladium nanoclusters of various forms [10] suggests higher reactivity of Pd–P nanoparticles (P : Pd = 0.3) in hydrogenation of alkynols, alkynes, and alkenes.

Based on the data obtained, we believe that the modifying effect of phosphorus on the properties of Pd–P particles in hydrogenation is due not only to the geometrical, but also to the electronic factor, which changes the energy of interaction of the active sites of Pd–P particles with the reaction participants. This assumption is based on the following facts.

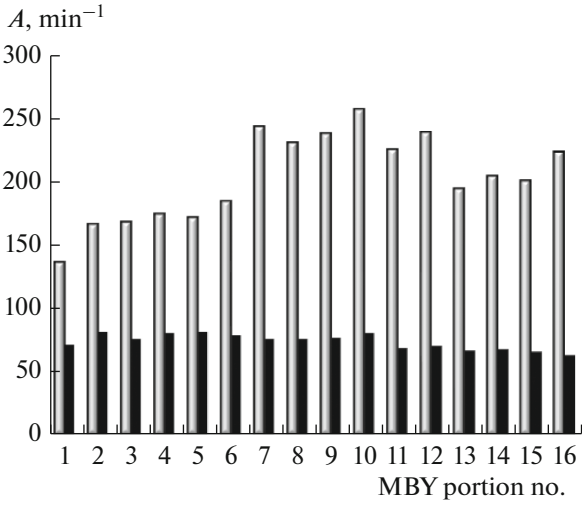

Fig. 5. Hydrogenation of the first 16 portions of 2-methyl-3-butyn-2-ol (gray column) and the resulting 2-methyl-3-butene-2-ol (black column) under the action of the Pd–P catalyst, P : Pd = 0.5. Reaction conditions: C_{Pd} = 2 mmol/L; one portion of MBY is 6.64×10^{-3} mol; DMF solvent, 10 mL, T = 30°C, P_{H_2} = 2 atm.

The preserved high alkenol selectivity of Pd–P nanoparticles at 96–98% conversion of the substrate shows that the selectivity depends not only on the ratio of hydrogenation rates of the competing substrates, but also on the ratio of the constants of adsorption equilibrium of the competing substrates (alkynol, alkenol) and the catalyst. As is known, the selectivity of palladium catalysts during triple bond hydrogenation is determined by the adsorption of alkyne, which is stronger than that of alkene or alkane [3]. For hydrogenation to occur, the adsorption of the reacting substances should not be too strong. According to the XPS data, at low P : Pd ratios (P : Pd = 0.3), the Pd(0) clusters that prevail on the surface of Pd–P particles are characterized by lower binding energies ($E_b(Pd3d_{5/2})$ = 334.5 eV) [25] compared with the binding energy of the bulk metal ($E_b(Pd3d_{5/2})$ = 335.2 eV) [31]. Pd catalysts with a high electron density on palladium are generally more active in the hydrogenation of unsaturated compounds [32, 33]. On the one hand,

Table 2. Effect of the precursor on the activity and selectivity of Pd–P nanoparticles in the hydrogenation of 2-methyl-3-butyn-2-ol*

Precursor	Activity (A), min^{-1}		$A_1 : A_2$	Conversion, %	Selectivity for MBE, %
	−C≡C−	−C=C−			
$Pd(OAc)_2$	166	127	1.3	97.2	95.6
$PdCl_2$	91	91	1.0	98.0	95.5
$Pd(acac)_2$	163	113	1.4	96.2	96.1

* Reaction conditions: C_{Pd} = 2 mmol/L, P : Pd = 0.5, $\nu_{MBY} = 6.64 \times 10^{-3}$ mol; DMF solvent, volume 10 mL, T = 30°C; P_{H_2} = 2 atm.

Table 3. Turnover frequencies of palladium catalysts formed from $Pd(acac)_2$ in the hydrogenation of MBY*

Catalyst	P : Pd	$C_{Pd(acac)_2}$, mmol/L	Particle size, nm		D_{TEM}	TOF, min^{-1}		
			d	d_{TEM}		MBY	PhA**	styrene
Pd black	0	1	22.2 ± 4.5	23.4	0.045	1300	444	666
Pd–P particles	0.1	1	5.9 ± 1.0	6.0	0.169	1189	911	1118
	0.1	2	10.7 ± 2.3	11.7	0.090	1444	942	–
	0.3	1	5.5 ± 0.9	5.65	0.187	1497	850	1497
	0.3	0.5	5.5 ± 0.9	5.65	0.187	2326	–	–
	0.3	0.25	5.5 ± 0.9	5.65	0.187	2380	–	–
$Pd(acac)_2$–$4AlEt_3$	0	5	2.45 ± 0.64	2.53	0.418	430	279	430
	0	2	2.45 ± 0.64	2.53	0.418	464	–	–
	0	0.5	2.45 ± 0.64	2.53	0.418	794	–	–
$Pd(acac)_2$–$6AlEt_3$	0	5	1.55 ± 0.57	1.65	0.604	382	201	264
	0	0.5	1.55 ± 0.57	1.65	0.604	607	–	–

The dash means that hydrogenation of PhA and styrene was not performed at these concentrations.
*For conditions, see Tables 1 and 2 and Fig. 2.
** PhA is phenylacetylene.

an excess of electrons on palladium atoms facilitates the dissociative chemisorption of the hydrogen molecule [32, 33]. On the other hand, it reduces the adsorption of both alkynes and alkenes, while the adsorption of alkenes is suppressed to a greater extent than that of alkynes [3]. Monosubstituted alkynes and alkynols are characterized by an extremely high adsorption affinity for palladium. Therefore, an increase in electron density on Pd(0) in Pd–P particles (P : Pd = 0.3) and, as a consequence, a decrease in the sorption affinity of alkynes (alkynols) should promote the growth of the catalytic activity. An increase in the selectivity and activity of Pd–Zn bimetallic alloys in the hydrogenation of 2-methyl-3-butyn-2-ol as a result of a decrease in the absolute values of the adsorption equilibrium constants K_{MBY} and K_{MBE} and a 1.4-fold increase in the K_{MBY}/K_{MBE} ratio compared with the corresponding values of the Lindlar catalyst was reported in [34].

This conclusion can explain the high TOF values of Pd–P particles only if the carriers of the catalytic activity are Pd(0) clusters. However, the Pd–P particles obtained by the low-temperature method contain both Pd(0) clusters and palladium phosphides, which contain the electron-deficient form of palladium ($Pd^{\delta+}$). Palladium-enriched palladium phosphides can also be active in hydroprocesses [35–37]. In order to determine which of the two forms (or both) is responsible for the catalytic properties of Pd–P nanoparticles in the hydrogenation of alkynols under mild conditions, additional experiments were performed.

Figure 3 presents the results of the formal kinetic study of MBY hydrogenation in the presence of the most active Pd–P particles (P : Pd = 0.3). The extremal dependence of the hydrogenation rate on the MBY concentration in the range 0.6–1.4 mmol/L indicates the competitive adsorption of MBY and hydrogen molecules at the active sites of Pd–P particles. The nearly zero concentration order of the reaction for MBY in the concentration range 0.6–1.05 M, as well as the first order for hydrogen ($n(H_2) = 1.04$), under mild reaction conditions (1–2 atm) suggest that the catalyst surface is saturated with the substrate and hydrogen is involved in the limiting stage of the reaction. Therefore, to describe the heterogeneous catalytic hydrogenation of 2-methyl-3-butyn-2-ol in the presence of Pd–P particles, we used the Langmuir–Hinshelwood mechanism, according to which activation of both hydrogen and MBY is necessary for the chemical reaction to proceed. The hydrogenation of 2-methyl-3-butyn-2-ol according to the Langmuir–Hinshelwood mechanism implies the competitive [38, 39] or noncompetitive [34] adsorption between hydrogen and MBY molecules at the active sites of the catalyst. The Rideal–Eley mechanism, which includes the activation of only one reagent [40], was not considered in this case.

Various kinetic models of the Langmuir–Hinshelwood mechanism for hydrogenation were presented in [41]. As the surface of Pd–P nanoparticles contains two potentially active forms of palladium, the following kinetic models are most likely (Table 4):

1. Hydrogenation proceeds between the previously adsorbed MBY and hydrogen molecules at active sites

Table 4. Kinetic models of hydrogenation of 2-methyl-3-butyn-2-ol by the Langmuir–Hinshelwood mechanism [41]

No.	Kinetic model	Kinetic equation*	Note
1	$MBY + \theta_o \xrightleftharpoons{K_{MBY}} \theta_{MBY}$; $H_2 + 2\theta_o \xrightleftharpoons{K_{H_2}} 2\theta_H$; $\theta_{MBY} + 2\theta_H \xrightarrow{k_1} \theta_{MBE} + 2\theta_o$; $r_1 = k_1\theta_{MBY}\theta_H^2$	$r_1 = k_1 \dfrac{K_{MBY}C_{MBY}K_{H_2}P_{H_2}}{\left(1 + K_{H_2}^{1/2}P_{H_2}^{1/2} + K_{MBY}C_{MBY}\right)^3}$	$\theta_H = \dfrac{K_{H_2}^{1/2}P_{H_2}^{1/2}}{\left(1 + K_{H_2}^{1/2}P_{H_2}^{1/2} + K_{MBY}C_{MBY}\right)}$ $\theta_{MBY} = \dfrac{K_{MBY}C_{MBY}}{1 + K_{H_2}^{1/2}P_{H_2}^{1/2} + K_{MBY}C_{MBY}}$
2	$MBY + \theta_o \xrightleftharpoons{K_{MBY}} \theta_{MBY}$; $H_2 + 2\theta'_o \xrightleftharpoons{K'_{H_2}} 2\theta'_H$ $\theta_{MBY} + 2\theta'_H \xrightarrow{k_1} \theta_{MBE} + 2\theta'_o$ $r_1 = k_1\theta_{MBY}(\theta'_H)^2$	$r_1 = k_1 \dfrac{K_{MBY}C_{MBY}K'_{H_2}P_{H_2}}{\left(1 + K_{MBY}C_{MBY} + K_{H_2}^{1/2}P_{H_2}^{1/2}\right)\left(1 + (K'_{H_2})^{1/2}P_{H_2}^{1/2}\right)^2}$	$\theta'_H = \dfrac{(K'_{H_2})^{1/2}P_{H_2}^{1/2}}{\left(1 + (K'_{H_2})^{1/2}P_{H_2}^{1/2}\right)}$ $\theta_{MBY} = \dfrac{K_{MBY}C_{MBY}}{1 + K_{H_2}^{1/2}P_{H_2}^{1/2} + K_{MBY}C_{MBY}}$
3	$MBY + \theta_o \xrightleftharpoons{K_{MBY}} \theta_{MBY}$; $H_2 + 2\theta'_o \xrightleftharpoons{K'_{H_2}} 2\theta'_H$ $\theta_{MBY} + 2\theta'_H \xrightarrow{k_1} \theta_{MBE} + 2\theta'_o$ $r_1 = k_1\theta_{MBY}(\theta'_H)^2$	$r_1 = k_1 \dfrac{K_{MBY}C_{MBY}K'_{H_2}P_{H_2}}{\left(1 + (K'_{H_2})^{1/2}P_{H_2}^{1/2} + K'_{MBY}C_{MBY}\right)^2(1 + K_{MBY}C_{MBY})}$	$\theta'_H = \dfrac{K_{H_2}^{1/2}P_{H_2}^{1/2}}{\left(1 + (K'_{H_2})^{1/2}P_{H_2}^{1/2} + K'_{MBY}C_{MBY}\right)}$ $\theta_{MBY} = \dfrac{K_{MBY}C_{MBY}}{(1 + K_{MBY}C_{MBY})}$
4	$H_2 + 2\theta_o \xrightarrow{k_{H_2}} 2\theta_H$ $MBY + \theta_o \xrightleftharpoons{K_{MBY}} \theta_{MBY}$ $r_1 = k_{H_2}\theta_o^2P_{H_2}$	$r_1 = \dfrac{k_{H_2}P_{H_2}}{(1 + K_{MBY}C_{MBY})^2}$	$\theta_o = \dfrac{1}{(1 + K_{MBY}C_{MBY})}$
5	$MBY + \theta_o \xrightarrow{k_{MBY}} \theta_{MBY}$ $H_2 + 2\theta_o \xrightleftharpoons{K_{H_2}} 2\theta_H$ $r_1 = k_{MBY}C_{MBY}\theta_o$	$r_1 = \dfrac{k_{MBY}C_{MBY}}{\left(1 + K_{H_2}^{1/2}P_{H_2}^{1/2}\right)}$	$\theta_o = \dfrac{1}{\left(1 + K_{H_2}^{1/2}P_{H_2}^{1/2}\right)}$

* The competitive adsorption between MBY and formed MBE is neglected in an assumption of weaker adsorption of MBE (models 1–5). The adsorption of hydrogen (model 4) or MBY (model 5) is neglected for the same reason.

of the same nature (competitive adsorption); the limiting stage is the surface reaction (model 1).

2. Hydrogenation occurs between the preliminarily adsorbed MBY and hydrogen molecules at different active sites (noncompetitive adsorption), but hydrogen can be adsorbed at the same sites as MBY; the limiting stage is the surface reaction (model 2).

3. Hydrogenation proceeds between the preliminarily adsorbed MBY and hydrogen molecules at different active sites (noncompetitive adsorption), but MBY can be adsorbed at the same sites as hydrogen; the limiting stage is the surface reaction (model 3).

4. The limiting stage is chemisorption of the hydrogen molecule (model 4).

5. The limiting stage is MBY adsorption (model 5).

At initial MBY concentrations higher than 0.6 M, a decrease in the reaction rate makes it possible to exclude kinetic models 2 and 5 from consideration; for these models, the initial reaction rate should increase continuously with an increase in the initial MBY concentration (linearly for model 5 and nonlinearly for model 2) (Table 4). For models 1, 3, and 4, the initial reaction rate decreases in the range of certain MBY concentrations [41]. The hydrogen chemisorption (model 4) evidently cannot be the limiting stage of MBY hydrogenation in the presence of Pd–P particles as the reaction rate in this case will decrease with increasing initial MBY concentrations. Thus, of the five proposed models, model 1 or 3 remains.

To answer the question of whether both potentially active forms of palladium (palladium nanoclusters and palladium phosphides) or only one of them (models 1 and 3) are involved in the hydrogenation of 2-methyl-3-butyn-2-ol, a combination of kinetic methods was proposed, which use the differential selectivity of catalytic systems as the main measured parameter under conditions of competition of several substrates.

In contrast to the catalytic activity, the differential selectivity at the same degrees of conversion is independent of the concentration of the active component of the catalyst and is determined by its nature [42, 43]. However, this condition is satisfied only when the products formed on one catalyst have the same orders of magnitude in the catalyst concentration [43]. The postulate about the identity of active sites on which the products are formed is fulfilled if competitive hydrogenation is performed for two substrates of the same type that differ in the substituent that is remote from the reaction site [43]. A simple method for evaluating the differential selectivity was proposed in [42, 43], in which it was suggested that the phase trajectories of the reaction that represent the mutual dependences of the product yields of the competing reactions should be used. The slope to any point on the phase trajectory equals the ratio of the product accumulation rates in the competing reactions, which unambiguously defines the differential selectivity.

An analysis of the results of competitive hydrogenation of two substrates of the same type presented in the form of phase trajectories will make it possible to differentiate the above-proposed models 1 and 3 at high probability. The coincidence of phase trajectories for different palladium catalysts indicates that the differential selectivities coincide and the nature of active sites is the same [43]. It should be borne in mind, however, that this result is still not an unambiguous proof of the identical nature of the catalyst. If the selectivity proved insensitive to a change in the nature of the catalyst, the result would be apparent constancy of selectivity with allowance for the experimental accuracy of its determination. If, however, the phase trajectories again coincide when the process parameters are varied, the nature of the active sites is the same. The noncoincidence of the phase trajectories of competitive hydrogenation of two substrates of the same type indicates that the nature of the active sites of the catalysts differs [43]. In view of the foregoing, two related acetylene alcohols were selected for competitive hydrogenation: 2-methyl-3-butyn-2-ol and 3-methyl-1-pentyn-3-ol.

The preliminary parallel experiments of competitive hydrogenation of MBY and MPY in the presence of various palladium catalysts showed good reproducibility. The almost complete coincidence of the phase trajectories of the parallel experiments on competitive hydrogenation of two acetylene alcohols in the presence of Pd black (Fig. 6a), colloidal solutions of Pd–P nanoparticles (Fig. 6b), or Ziegler systems (Fig. 7) allows us to exclude the effect of reproducibility of the heterogeneous catalytic experiments on discrimination of hypotheses and to proceed to the analysis of phase trajectories for various palladium catalysts. It should be emphasized that the phase trajectories constructed according to the accumulation of the products of competing reactions (allyl or saturated alcohols) and according to the decrease in the concentrations of competing acetylene alcohols coincided in the parallel experiments (Fig. 6b). At the same time, the similar phase trajectories of competitive hydrogenation of MBY and MPY in the presence of Pd–P nanoparticles and Pd black diverge (Fig. 8). At a first glance, it could be suggested that of the two potential forms (Pd(0) clusters and palladium phosphides), palladium phosphides are active in the hydrogenation of alkynols. However, as hydrogenation of alkynols is a size-sensitive reaction [11, 12] and the sizes of Pd–P nanoparticles (d = 5.9 nm) and Pd black (d = 22 nm) significantly differ, additional experiments were performed on the competitive hydrogenation of MBY and MPY in the presence of smaller palladium nanoclusters (Fig. 4). The catalysts were Ziegler systems, in which the size of palladium nanoclusters can be relatively easily adjusted by varying the ratio of the organoaluminum cocatalyst to the palladium precursor [30].

A comparison of the phase trajectories of the competitive hydrogenation of acetylene alcohols (MBY

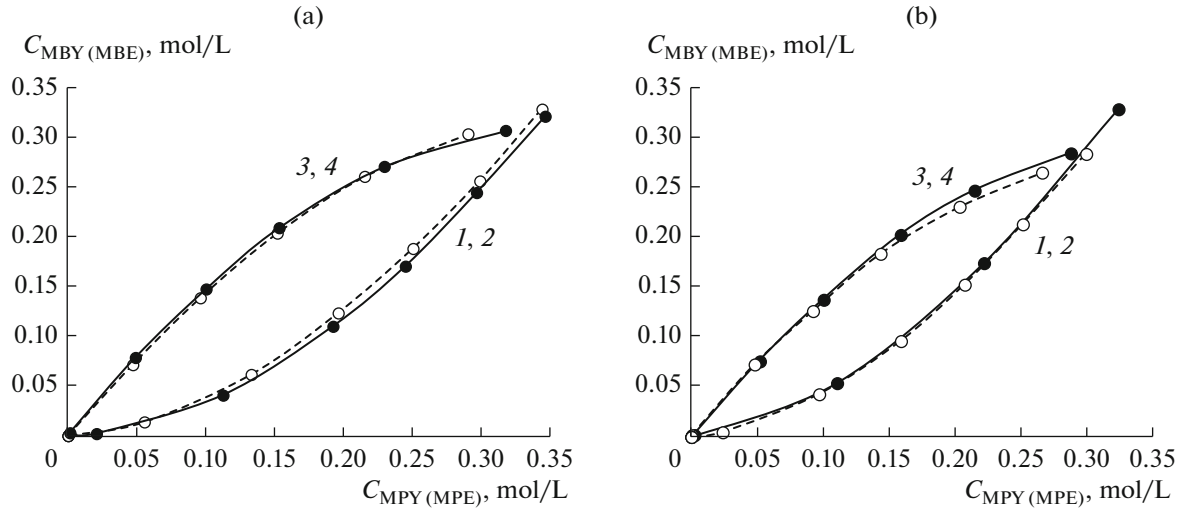

Fig. 6. Phase trajectories of parallel experiments on the (*1*, *2*) competitive hydrogenation of two alkynols (MBY, MPY) and (*3*, *4*) formation of allyl alcohols (MBE, MPE) in the presence of (a) Pd black and (b) Pd–P nanoparticles (P : Pd = 0.3). Reaction conditions: (a) C_{Pd} = 1.0 mmol/L, (b) C_{Pd} = 0.5 mmol/L, T = 30°C, P_{H_2} = 2 atm, DMF solvent, 10 mL.

and MPY) in the presence of Pd–P nanoparticles and Ziegler systems gave an unexpected result. The phase trajectories of competitive hydrogenation constructed according to the decrease in the MBY and MPY concentrations coincide, while those constructed according to the concentrations of the reaction products diverge; i.e., the ratios of the hydrogenation rates of alkynols coincide, while the ratios of the accumulation (formation and consumption) rates of ethylene alcohols differ (Fig. 9). The coincidence of the phase trajectories of the competitive hydrogenation of acetylene alcohols suggests, at high probability, that the nature of active sites in these catalysts is identical. Therefore, of the two potentially active sites contained in Pd–P nanoparticles, the Pd(0) clusters exhibit activity in the hydrogenation of alkynols.

The noncoincidence of the phase trajectories of the formed ethylene alcohols could be the result of the

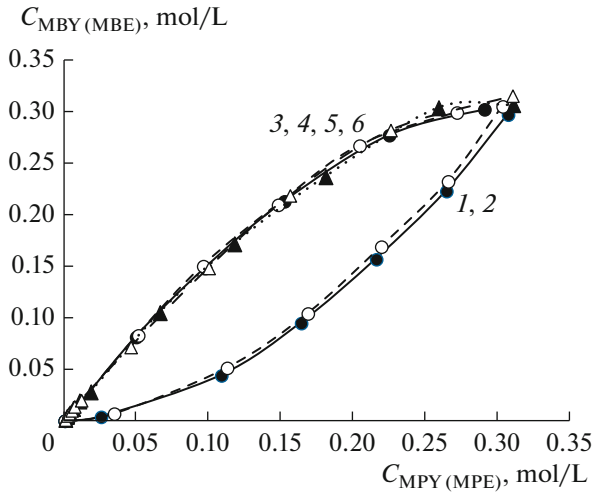

Fig. 7. Phase trajectories of parallel experiments on the competitive hydrogenation of (*1*, *2*) two acetylene alcohols (MBY, MPY) and formation of (a) (*3*, *4*) allyl (MBE, MPE) and (b) (*5*, *6*) saturated (MBA, MPA) alcohols in the presence of the $Pd(acac)_2$–$6AlEt_3$ system. Reaction conditions: C_{Pd} = 0.5 mmol/L, T = 30°C, P_{H_2} = 2 atm, toluene solvent, 10 mL.

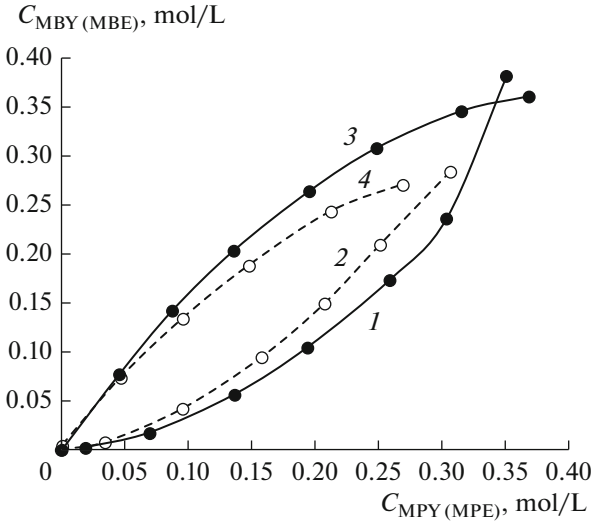

Fig. 8. Phase trajectories of the (*1*, *2*) competitive hydrogenation of alkynols (MBY, MPY) and (*3*, *4*) formation of allyl alcohols (MBE, MPE) in the presence of (*1*, *3*) Pd black and (*2*, *4*) Pd–P nanoparticles (P : Pd = 0.3). Reaction conditions: T = 30°C, P_{H_2} = 2 atm, DMF solvent, 10 mL.

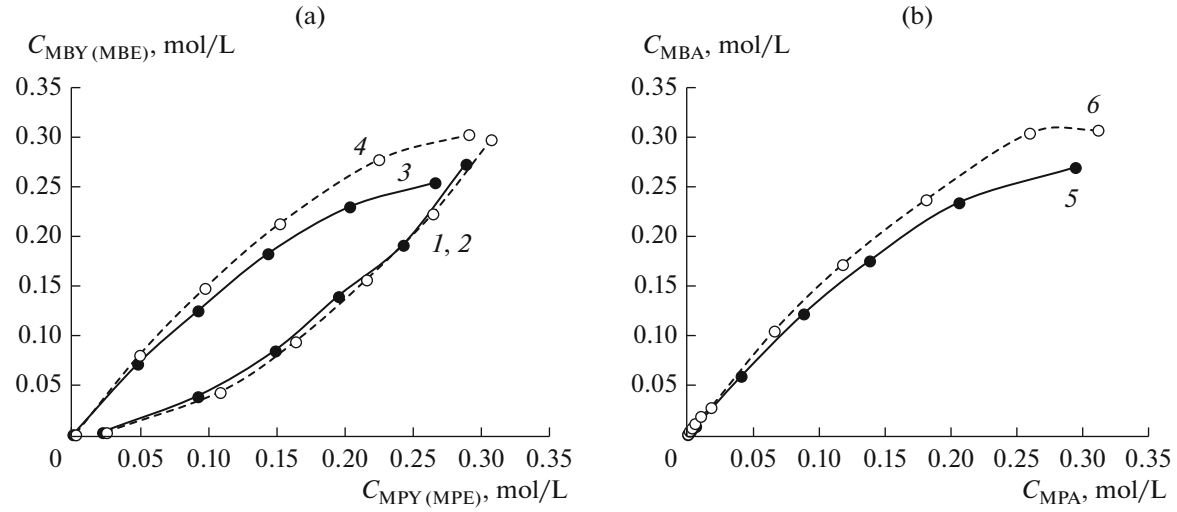

Fig. 9. Phase trajectories of the (*1*, *2*) competitive hydrogenation of alkynols (MBY, MPY), and (*3*, *4*) formation of (a) allyl (MBE, MPE) and (b) (*5*, *6*) saturated alcohols (MBA, MPA) in the presence of (*1*, *3*, *5*) Pd–P nanoparticles (P : Pd = 0.3) and (*2*, *4*, *6*) $Pd(acac)_2$–$6AlEt_3$ system. Reaction conditions: $T = 30°C$, $P_{H_2} = 2$ atm.

conversion of alkynols into the by-products (of dimerization and isomerization). However, this is excluded in view of the coincidence of the phase trajectories constructed according to the sums of the conversion products of alkynols (allyl and saturated alcohols). Therefore, the observed difference between the phase trajectories of the competitive hydrogenation of acetylene alcohols (MBY and MPY) constructed according to allyl alcohols is associated with their further saturation. If the unsaturated alcohols remained the final products, the phase trajectories constructed according to both the decrease in the concentration of acetylene alcohols and accumulation of their hydrogenation products would coincide.

As is known, hydrogenation can involve not only hydrogen of the surface layer, but also hydrogen of the near-surface layer called "nonselective" [1], which saturates alkynes to alkanes without their desorption stage. The contribution of "nonselective" hydrogen can be neglected in view of the lower solubility of hydrogen in small palladium clusters [44] and palladium phosphides compared with that in bulk palladium [45], and also taking into account the low proportion of 2-methylbutan-2-ol and 3-methylpentan-3-ol during the hydrogenation of alkynols (Fig. 1).

An analysis of the phase trajectories of the competitive hydrogenation of MBY and MPY suggests that the hydrogenation of alkynols in the presence of Pd–P nanoparticles most likely proceeds on Pd(0) clusters, and further saturation of allyl alcohols occurs on both types of active sites: Pd(0) clusters and palladium phosphide. Of the two types of active sites, the reaction mainly proceeds on those sites that are characterized by the lower activation energy. The *d* metal phosphides are generally less active than metal catalysts in hydrogenation catalysis, but more resistant to deactivation [46, 47]. The hydrogenation requires the activation of both molecular hydrogen and substrate. As the partial positive charge on palladium in palladium phosphide ($E_b(Pd3d_{5/2}) = 336.1$ eV) [25] is unfavorable for the activation of molecular hydrogen, hydrogen chemisorption evidently predominantly occurs on Pd(0) clusters, while the adsorption of allyl alcohols occurs on both Pd(0) clusters and palladium phosphides. Palladium phosphides show activity in the presence of the more active form—Pd(0) clusters—probably because of the partial transfer of hydrogen by the spillover mechanism from Pd(0) clusters to allyl alcohol adsorbed on palladium phosphide and its subsequent saturation.

CONCLUSIONS

A method was proposed for the preparation of an effective catalyst for hydrogenation of alkynols, which surpasses the known palladium nanoclusters in its activity and retains high selectivity (95–96%) at 97–98% substrate conversion. The promoting effect of phosphorus on the properties of the palladium catalyst is due not only to an increase in dispersion, but also to higher reactivity of Pd–P particles. An analysis of the differential selectivity of various palladium catalysts shows that of the two types of active sites contained in Pd–P particles, hydrogenation of alkynols most likely occurs on Pd(0) clusters, and further saturation of allyl alcohols occurs on both Pd(0) clusters and palladium phosphide.

FUNDING

This study was performed under the government contract in the field of research and development of the Russian Ministry of Education and Science (no. 4.9489.2017/8.9). The electronic images of the catalyst samples were obtained on the electron microscope of the Multiaccess Center, Baikal Center for Nanotechnology, Irkutsk National Research Technical University.

REFERENCES

1. Vile, G., Albani, D., Almora-Barrios, N., Lopez, N., and Perez-Ramirez, J., *ChemCatChem*, 2016, vol. 8, p. 21.
2. McCue, A.J. and Anderson, J.A., *Front. Chem. Sci. Eng.*, 2015, vol. 9, no. 2, p. 142.
3. Nikolaev, S.A., Smirnov, V.V., Zanaveskin, L.N., Zanaveskin, K.L., and Averyanov, V.A., *Russ. Chem. Rev.*, 2009, vol. 78, no. 3, p. 231.
4. Stolarov, I.P., Yakushev, I.A., Churakov, A.V., Cherkashina, N.V., Smirnova, N.S., Khramov, E.V., Zubavichus, Y.V., Khrustalev, V.N., Markov, A.A., Klyagina, A.P., Kornev, A.B., Martynenko, V.M., Gekhman, A.E., Vargaftik, M.N., and Moiseev, I.I., *Inorg. Chem.*, 2018, vol. 57, no. 18, p. 11482.
5. Johnston, S.K., Cherkasov, N., Pérez-Barrado, E., Aho, A., Murzin, D.Y., Ibhadon, A.O., and Francesconi, M. G., *Appl. Catal., A,* 2017, vol. 544, p. 40.
6. Nikoshvili, L., Bykov, A., Khudyakova, T., LaGrange, T., Héroguel, F., Luterbacher, J.S., Matveeva, V.G., Sulman, E.M., Dyson, P.J., and Kiwi-Minsker, L., *Ind. Eng. Chem. Res.*, 2017, vol. 56, p. 45.
7. Maki-Arvela, P., Hajeк, I., Salmi, T., and Murzin, D.Yu., *Appl. Catal., A*, 2005, vol. 292, p. 1.
8. Wu, W., Zhang, W., Long, Y., Qin, J., Wen, H., and Ma, J., *J. Colloid Interface Sci.*, 2018, vol. 531, p. 642.
9. Directive 2002/95/EC of the European Parliament and of the Council of 27 January 2003 on the restriction of the use of certain hazardous substances in electrical and electronic equipment, *Official J. L.*, 2002, vol. 37, p. 13.
10. Crespo-Quesada, M., Yarulin, A., Jin, M., Xia, Y., and Kiwi-Minsker, L., *J. Am. Chem. Soc.*, 2011, vol. 133, p. 12787.
11. Markov, P.V., Mashkovsky, I.S., Bragina, G.O., Warn, J., Gerasimov, E.Yu., Bukhtiyarov, V.I., Stakheev, A.Yu., and Murzin, D.Yu., *Chem. Eng. J.*, 2019, vol. 358, p. 520.
12. Yarulin, A.E., Crespo-Quesada, R.M., Egorova, E.V., and Kiwi-Minsker, L.L., *Kinet. Catal.,* 2012, vol. 53, no. 2, p. 253.
13. Vorobyeva, E., Chen, Z., Mitchell, S., Leary, R.K., Midgley, P., Thomas, J.M., Hauert, R., Fako, E., Lopez, N., and Perez-Ramırez, J., *J. Mater. Chem. A*, 2017, vol. 5, p. 16393.
14. Okhlopkova, L.B., Cherepanova, S.V., Prosvirin, I.P., Kerzhentsev, M.A., and Ismagilov, Z.R., *Appl. Catal., A*, 2018, vol. 549, p. 245.
15. Shen, L., Mao, S., Li, J., Li, M., Chen, P., Li, H., Chen, Z., and Wang, Y., *J. Catal.*, 2017, vol. 350, p. 13.
16. Mashkovsky, I.S., Baeva, G.N., Stakheev, A.Y., Vargaftik, M.N., Kozitsyna, N.Y., and Moiseev, I.I., *Mendeleev Commun.*, 2014, vol. 24, p. 355.
17. Shlyapin, D.A., Glyzdova, D.V., Afonasenko, T.N., Temerev, V.L., and Tsyrul'nikov, P.G., *Kinet. Catal.,* 2019, vol. 60, no. 4, p. 446.
18. Guo, M., Li, H., Ren, Y., Ren, X., Yang, Q., and Li, C., *ACS Catal.*, 2018, vol. 8, p. 6476.
19. Vargaftik, M.H., Kozitsyna, N.Yu., Cherkashin, N.V., Rudyi, R.I., Kochubei, D.I., Novgorodov, B.N., and Moiseev, I.I., *Kinet. Catal.,* 1998, vol. 39, no. 6, p. 740.
20. Shmidt, F.K., Belykh, L.B., and Cherenkova, T.V., *Kinet. Catal.*, 2001, vol. 42, no. 2, p. 163.
21. Belykh, L.B., Skripov, N.I., Belonogova, L.N., Umanets, V.A., and Schmidt, F.K., *Kinet. Catal.,* 2010, vol. 51, no. 1, p. 42.
22. Skripov, N.I., Belykh, L.B., Belonogova, L.N., Umanets, V.A., Ryzhkovich, E.N., and Schmidt, F.K., *Kinet. Catal.,* 2010, vol. 51, no. 5, p. 714.
23. Skripov, N.I., Belykh, L.B., Sterenchuk, T.P., Akimov, V.V., Tauson, V.L., and Schmidt, F.K., *Kinet. Catal.,* 2017, vol. 58, no. 1, p. 34.
24. Belykh, L.B., Sterenchuk, T.P., Skripov, N.I., Akimov, V.V., Tauson, V.L., Romanchenko, A.S., Gvozdovskaya, K.L., Sanzhieva, K.L., and Schmidt, F.K., *Kinet. Catal.,* 2019, vol. 60, no. 6, p. 808.
25. Belykh, L.B., Skripov, N.I., Sterenchuk, T.P., Schmidt, F.K., Akimov, V.V., and Tauson, V.L., *Russ. J. Gen. Chem.*, 2016, vol. 86, no. 9, p. 2022.
26. Gordon, A.J. and Ford, R.A., *The Chemist's Companion: A Handbook of Practical Data, Techniques, and References*, Hoboken: Wiley, 1972, p. 560.
27. Matthews, J.C., Nashua, N.H., and Wood, L.L., US Patent 3474464, 1969.
28. Ott, L.S. and Finke, R.G., *Coord. Chem. Rev.*, 2007, vol. 251, nos. 9–10, p. 1075.
29. Shmidt, F.K., Titova, Yu.Yu., and Belykh, L.B., *Kinet. Catal.,* 2015, vol. 56, no. 5, p. 574.
30. Belykh, L.B., Titova, Yu.Yu., Umanets, V.A., and Shmidt, F.K., *Russ. J. Appl. Chem.*, 2006, vol. 79, no. 8, p. 1271.
31. Tsyrul'nikov, P.G., Afonasenko, T.N., Koshcheev, S.V, and Boronin, A.I., *Kinet. Catal.,* 2007, vol. 48, no. 5, p. 728.
32. Mironenko, R.M., Belskaya, O.B., Lavrenov, A.V., and Likholobov, V.A., *Kinet. Catal.,* 2018, vol. 59, no. 3, p. 339.
33. Maccarrone, M.J., Lederhos, C.R., Torres, G., Betti, C., Coloma-Pascual, F., Quiroga, M.E., and Yori, J.C., *Appl. Catal., A,* 2012, vols. 441–442, p. 90.
34. Vernuccio, S., Goy, R., Rohr, Ph.R., Medlock, J., and Bonrath, W., *React. Chem. Eng.*, 2016, vol. 1, p. 445.
35. Carenco, S., Leyva-Perez, A., Concepciyn, P., Boissiere, C., Mezailles, N., Sanchez, C., and Corma, A., *Nano Today*, 2012, vol. 7, p. 21.
36. Oyama, S.T., Gott, T., Zhao, H., and Lee, Y.K., *Catal. Today*, 2009, vol. 143, nos. 1–2, p. 94.
37. d'Aquino, A.I., Danforth, S.J., Clinkingbeard, T.R., Ilic, B., Pullan, L., Reynolds, M.A., Murray, B.D., and Bussel, M.E., *J. Catal.*, 2016, vol. 335, p. 204.

38. Semagina, N., Grasemann, M., Xanthopoulos, N., Renken, A., and Kiwi-Minsker, L., *J. Catal.*, 2007, vol. 251, p. 213.
39. Crespo-Quesada, M., Grasemann, M., Semagina, N., Renken, A., and Kiwi-Minsker, L., *Catal. Today*, 2009, vol. 147, nos. 3–4, p. 247.
40. Protasova, L.N., Rebrov, E.V., Choy, K.L., Pung, S.Y., Engels, V., Cabaj, M., Wheatley, A.E.H., and Schouten, J.C., *Catal. Sci. Technol.*, 2011, vol. 1, p. 768.
41. Serna, P., Concepción, P., and Corma, A., *J. Catal.*, 2009, vol. 265, p. 19.
42. Schmidt, A.F., Kurokhtina, A.A., and Larina, E.V., *Catal. Sci. Technol.*, 2014, vol. 4, p. 3439.
43. Schmidt, A.F., Kurokhtina, A.A., and Larina, E.V., *Kinet. Catal.,* 2019, vol. 60, no. 5, p. 551.
44. Kobayashi, H., Yamauchi, M., Kitagawa, H., Kubota, Yo., Kato, K., and Takata, M., *J. Am. Chem. Soc.*, 2008, vol. 130, p. 1818.
45. Stojewski, M., Kowalska, J., and Jurczakowski, R., *J. Phys. Chem. C*, 2009, vol. 113, no. 9, p. 3707.
46. Prins, R. and Bussell, M.E., *Catal Lett.*, 2012, vol. 142, no. 12, p. 1413.
47. Zhao, M., *Chem. – Asian J.*, 2016, vol. 11, p. 461.

Translated by L. Smolina